

# Crystallized Rate Regions for Full Duplex Enabled Small Cell Networks

Radwa Sultan<sup>†</sup>, Karim G. Seddik\*, and Zhu Han<sup>†</sup>

<sup>†</sup> Electrical and Computer Engineering Department, University of Houston, TX, USA

\* Electronics and Communications Engineering Department, American University in Cairo, New Cairo, Egypt

**Abstract**—In this paper, we study full-duplex enabled small cell networks. We consider a two-node network, in which each node can operate in full-duplex. After treating interference as noise, we derive each node's achieved uplink and downlink rate, for both the half-duplex and full-duplex transmissions. Afterwards, the rate maximization problem used in obtaining the achieved rate region is formulated, and a very low complexity algorithm is proposed to obtain the crystallized rate regions. The idea is to explore the boundary points of the rate region and then find their convex hull. Finally, numerical analysis is presented to compare the exact achieved rate regions with the crystallized regions and to validate that the crystallized regions can approximate the exact regions with much less complexity. Also, in some cases, the rate region derived from power adaptation will be confined to the crystallized rate region; which suggests that in these cases, time-sharing will be more beneficial, in terms of data rates, than power adaptation.

## I. INTRODUCTION

The next generation cellular networks are required to offer a large performance boost in the achieved data rates. Accordingly, efficient resource utilization techniques are needed in order to meet these demands. A full-duplex (FD) transceiver can transmit and receive simultaneously on the same time and frequency resources. Theoretically speaking, enabling FD communications can double the achieved communication link's capacity. However, the main hurdle that prevents FD communications from achieving such high capacities is the high self-interference (SI) power from the transceiver's transmission at the transceiver's reception, which greatly degrades the received signal-to-interference noise ratio (SINR).

Recently, the evolution in SI cancellation techniques [1]–[3] revives the attention to FD communication and nominates the FD communication as a technique that is able to supply the needed high rates in the next generation networks [4]–[6]. Furthermore, studying FD communication in small cell networks (SCN) attracts recent research work. SCN [7]–[9] has emerged as a very promising network topology that is capable of providing capacity for both indoors and outdoors which helps provide the desired rise in data rates. Therefore, it is expected that deploying FD along with SCNs will provide a great enhancement of the network's performance. In [10], a study of the effect of FD on resource allocation for SCN is presented. A resource allocation problem is formulated to adjust the base station and the femtocell access point transmitting powers to maximize the downlink channel capacity while guaranteeing the uplink channel QoS by maintaining a certain channel capacity. The results show when it is preferable to

employ FD and when it is more advantageous to use half-duplex (HD). In [11], a switching criterion between FD and HD is proposed in FD-SCN. Subsequently, based on the study of the system's parameters that affect the performance of both FD and HD, theoretical switching thresholds for these parameters are derived. In [12], an FD orthogonal division multiple access (OFDMA) heterogeneous network is studied. A joint resource allocation problem, which maximizes the aggregate network's throughput by considering mode selection, user pairing, sub-carrier allocation and power control, is proposed.

Additionally, deriving achievable rate regions and studying the performance gains achieved from deploying FD have attracted recent research work. In [13], the authors propose a simple inter-user interference cancellation (IIC) scheme to deal with the inter-user interference (IUI), which results from the uplink (UL) transmission on the downlink (DL) transmission. Afterwards, the achievable rate region of the FD system with and without IIC are analyzed, when taking the SI into consideration. In [14], the relationship between accurate SI channel estimation and spectral-efficient simultaneous two-way data transmission and reception in a bidirectional FD radio link between a base station and a mobile user in a cellular network is analyzed. The analysis is conducted by deriving the achievable data rates and calculating the corresponding rate regions. Additionally, in [15], the rate regions of HD and FD links using the orthogonal frequency division multiplexing (OFDM) technique are analyzed after taking into account the non-ideality of practical transceivers, where two different optimal power allocation algorithms are developed. In the first, each node uniformly allocates the power over sub-carriers, and in the second one, each node adaptively allocates the power over sub-carriers to achieve the largest rate. However, it should be mentioned that the complexity of deriving the achieved rate regions is highly complicated.

In this paper, we study a two-nodes FD-enabled SCN. We propose a low-complexity scheme for deriving the crystallized rate regions. The idea of the crystallized rate region is proposed in [16]–[18]; it is proposed to simplify the calculation of achievable rate regions by considering a subset of users and power allocation and construct the convex hull of the rate region based on those combinations<sup>1</sup>. The combinations considered are those which most likely will lie on the boundary

<sup>1</sup>The convex hull, of a set  $X$  of points, is defined as the smallest convex set that contains  $X$ .

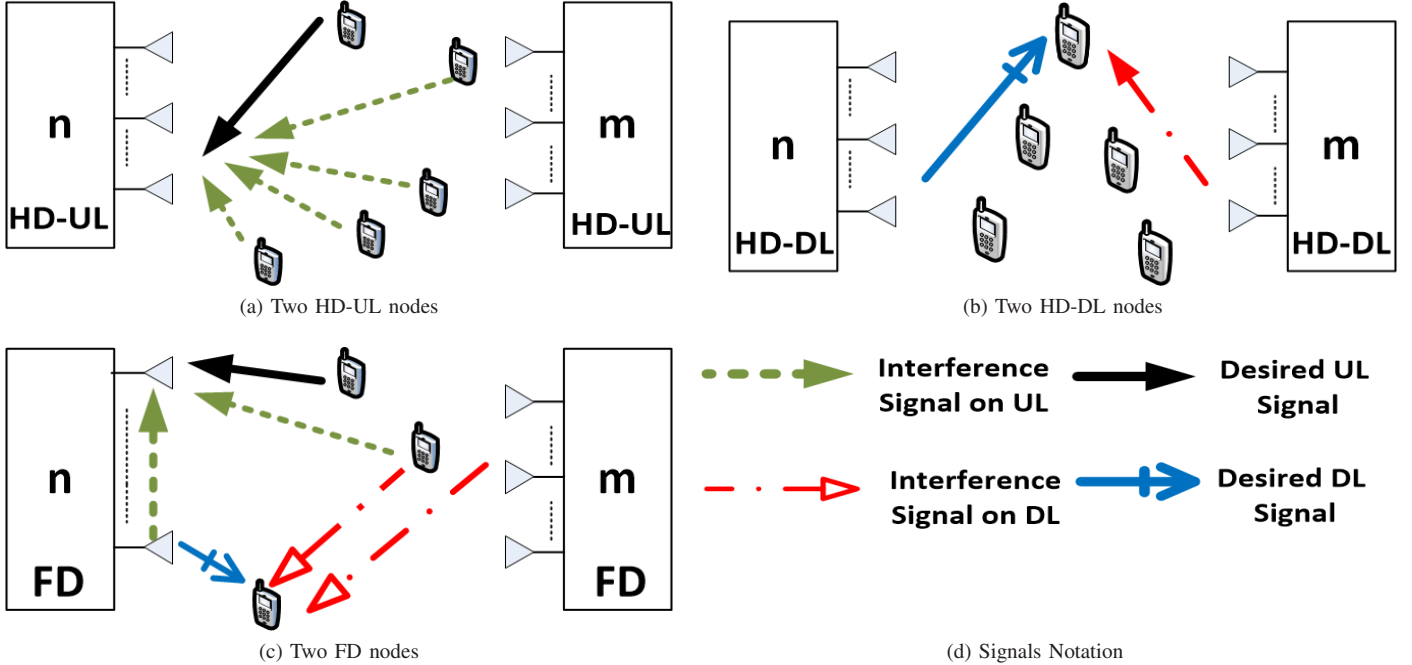


Fig. 1: Transmission and Interference Signal for all Possible Transmission Modes

of the feasible rate region and each rate point that lies on the convex hull could be achieved by time-sharing [16]<sup>2</sup>. The number of these combinations should not grow exponentially with the number of users. Our contributions in this paper are summarized as follows:

- Studying the HD and FD operation of a two-node network and deriving the rate maximization problem required for obtaining the achieved rate regions for HD and FD modes, in both the UL and DL transmissions.
- Proposing a low-complexity algorithm to derive the crystallized rate regions for HD and FD modes, in both the UL and DL transmissions.
- Validating, through extensive numerical analysis, that the crystallized rate regions can approximate the achieved rate regions with much less complexity.

The remainder of this paper is organized as follows. The system model is presented in Section II. Deriving the crystallized rate region is presented in Section III. Numerical analysis is presented in Section IV. Finally, the paper is concluded in Section V.

## II. SYSTEM MODEL

We present a SCN with two nodes ( $n, m$ ) each with  $M$  antennas; nodes  $n$  and  $m$  serve  $K_n$  and  $K_m$  users, respectively. Assume all nodes and users share the same time slot and frequency band. In this paper, we investigate the case where the node has the choice to work either in HD or FD. In the case of a HD node, all the node's antennas are dedicated either to

<sup>2</sup>As will become clear later in the paper, time-sharing can, in some cases, result in higher rates than those achieved by power adaptation; the same observation was made in [17] but in a different context.

transmission or reception. However, in the case of a FD node, half of the antennas are used for transmission and the other half are used for reception. In order to better understand how the network operates, Fig. 1 shows the transmission signals and interference signals for different cases of nodes' transmission modes. Based on the above assumption, the network will operate in one of the following two cases.

### A. Case 1. All Nodes Operate in HD

In this case, it is assumed that in the first time slot the UL transmissions take place. Therefore, as shown in Fig. 1a, the interference sources on each user will be caused from the other UL transmissions from all other UL users. Consequently, the received UL SINR at node  $n$  from the  $k^{\text{th}}$  user is given by

$$\Gamma_{ul|hd-hd} = \frac{P_k D_{kn}^{-\alpha} |\mathbf{h}_{nk}|^2}{\sigma^2 + \sum_{\substack{k'=1 \\ k' \neq k}}^{K_n+K_m} P_{k'} D_{k'n}^{-\alpha} |\mathbf{h}_{nk'}|^2}, \quad (1)$$

where  $P_k$  is the  $k^{\text{th}}$  user's UL transmission power,  $D_{kn}$  is the distance between the node  $n$  and user  $k$ ,  $\alpha$  is the path-loss exponent,  $\mathbf{h}_{nk} \in \mathbb{C}^{M \times 1}$  is the HD-UL channel vector between node  $n$  and user  $k$ <sup>3</sup>, all the channel coefficients are assumed to be an i.i.d. zero mean complex Gaussian random variables with unit variance, i.e., Rayleigh fading,  $\sigma^2$  represents the additive white Gaussian noise (AWGN) variance and the summation in the denominator, in (1), denotes the interference from all other users in the network. On the hand, in the second time slot, the DL transmissions take place. The interference signals are

<sup>3</sup>Throughout this paper,  $\mathbf{h}_{xy}$  denotes the channel vector between transmitter  $y$  and receiver  $x$ .

shown in Fig. 1b. Accordingly, the received DL SINR at the  $k^{th}$  user served by node  $n$  is given by

$$\Gamma_{dl|hd-hd} = \frac{P_n D_{kn}^{-\alpha} |\mathbf{h}_{kn} \mathbf{w}_{kn}|^2}{\sigma^2 + I_{dl|hd-hd}^n + I_{dl|hd-hd}^m}, \quad (2)$$

where  $\mathbf{h}_{kn} \in \mathbb{C}^{1 \times M}$  is the HD-DL channel between user  $k$  and node  $n$ ,  $\mathbf{w}_{kn} \in \mathbb{C}^{M \times 1}$  is the precoding vector for the DL transmission between user  $k$  and node  $n$ ,  $I_{dl|hd-hd}^n$  calculates the interference from all other DL transmissions from the same node  $n$ , while  $I_{dl|hd-hd}^m$  calculates the interference from the other DL transmissions from node  $m$ . The values of  $I_{dl|hd-hd}^n$  and  $I_{dl|hd-hd}^m$  are given, respectively, by

$$I_{dl|hd-hd}^n = \sum_{\substack{k'=1 \\ k' \neq k}}^{K_n} P_n D_{kn}^{-\alpha} |\mathbf{h}_{kn} \mathbf{w}_{k'n}|^2, \quad (3)$$

$$I_{dl|hd-hd}^m = \sum_{k'=1}^{K_m} P_m D_{km}^{-\alpha} |\mathbf{h}_{km} \mathbf{w}_{k'm}|^2.$$

Note that, both UL and DL SINRs for the users connected to node  $m$  can be derived from (1) and (2), respectively, after interchanging node  $n$  by node  $m$  and node  $m$  by node  $n$ . Therefore, UL and DL rates, for nodes  $n$  and  $m$ , per unit bandwidth will be equal, respectively, to

$$\begin{aligned} R_{hd-hd|n}^{ul} &= \log_2(1 + \Gamma_{ul|hd-hd}), \\ R_{hd-hd|m}^{ul} &= \log_2(1 + \Gamma_{ul|hd-hd}^{n \leftrightarrow m}), \\ R_{hd-hd|n}^{dl} &= \log_2(1 + \Gamma_{dl|hd-hd}), \\ R_{hd-hd|m}^{dl} &= \log_2(1 + \Gamma_{dl|hd-hd}^{n \leftrightarrow m}). \end{aligned} \quad (4)$$

where  $n \leftrightarrow m$  denotes the interchanging between nodes  $n$  and  $m$ .

### B. Case 2. All Nodes Operate in FD

In this case, each time slot will serve both UL and DL transmissions. Therefore, on average, the received UL and DL SINRs will be the same for the first and second time slots. Additionally, as illustrated in Fig. 1c, FD transmission suffers from SI which greatly affects the UL SINR. Therefore, special FD radio is needed in order to cancel the unwanted SI power. At the  $n^{th}$  node, therefore, the received UL SINR, from user  $k$ , is given by

$$\Gamma_{ul|fd-fd} = \frac{P_k D_{kn}^{-\alpha} |\mathbf{g}_{nk}|^2}{\sigma^2 + CP_n |\mathbf{G}_n \mathbf{V}_n|^2 + I_n + I_m}, \quad (5)$$

where  $\mathbf{g}_{nk} \in \mathbb{C}^{\frac{M}{2} \times 1}$  is the FD channel between node  $n$  and user  $k$ ,  $CP_n |\mathbf{G}_n \mathbf{V}_n|^2$  is the residual self-interference (RSI) power, where  $C$  as the SI cancellation coefficient,  $\mathbf{G}_n \in \mathbb{C}^{\frac{M}{2} \times \frac{M}{2}}$  is the channel between the node  $n$  transmitting and receiving antennas,  $\mathbf{V}_n \in \mathbb{C}^{\frac{M}{2} \times \frac{M}{2}}$  is node  $n$  FD precoding matrix,  $I_n$  is the interference power from all other UL transmissions, it is given by

$$I_n = \sum_{\substack{k'=1 \\ k' \neq k \\ k \in \Psi_{ul}}}^{K_n+K_m} P_{k'} D_{k'n}^{-\alpha} |\mathbf{g}_{nk'}|^2, \quad (6)$$

where  $\Psi_{ul}$  is the set of UL users in the given time slot, the last term in the denominator, in (5),  $I_m$  calculates the interference from node  $m$  DL transmission, it is given by

$$I_m = P_m D_{nm}^{-\alpha} |\mathbf{G}_{nm} \mathbf{V}_m|^2, \quad (7)$$

where  $D_{nm}$  is the distance between node  $n$  and node  $m$  and  $\mathbf{G}_{nm} \in \mathbb{C}^{\frac{M}{2} \times \frac{M}{2}}$  is the channel between node  $m$  transmitting antennas and node  $n$  receiving antennas. Additionally, the received DL SINR at the  $k^{th}$  user served by node  $n$  is given by

$$\Gamma_{dl|fd-fd} = \frac{P_n D_{kn}^{-\alpha} |\mathbf{g}_{kn} \mathbf{v}_{kn}|^2}{\sigma^2 + \sum_{\substack{k'=1 \\ k' \neq k \\ k' \in \Psi_{dl|n}}}^{K_n} I_{dl|n} + \sum_{\substack{k'=1 \\ k' \neq k \\ k' \in \Psi_{dl|m}}}^{K_m} I_{dl|m} + \sum_{\substack{k'=1 \\ k' \neq k \\ k \in \Psi_{ul}}}^{K_n+K_m} I_{ul}}, \quad (8)$$

where  $\Psi_{dl|n}$  and  $\Psi_{dl|m}$  are the set of DL users connected to node  $n$  and node  $m$ , respectively. The summation over  $I_{dl|n}$  calculates the interference from all other DL transmissions connected to node  $n$ , and is given by

$$I_{dl|n} = P_n D_{kn}^{-\alpha} |\mathbf{g}_{kn} \mathbf{v}_{k'n}|^2. \quad (9)$$

On the other hand,  $I_{dl|m}$  calculates the interference from all other DL transmissions connected to node  $m$ , and is given by

$$I_{dl|m} = P_m D_{km}^{-\alpha} |\mathbf{g}_{km} \mathbf{v}_{k'm}|^2; \quad (10)$$

the summation over  $I_{ul}$  calculates the interference from all UL transmissions connected to both nodes  $n$  and  $m$ , it is given by

$$I_{ul} = P_{k'} D_{k'k}^{-\alpha} |\mathbf{g}_{kk'}|^2. \quad (11)$$

Similarly, as in Section II-A, both UL and DL SINRs for users connected to node  $m$  can be derived from (5) and (8), respectively, after interchanging node  $n$  by node  $m$  and node  $m$  by node  $n$ . Therefore, the total rate in two successive time slots, per unit bandwidth in that case for node  $n$  and node  $m$  will be equal, respectively, to

$$\begin{aligned} R_{fd-fd|n}^{ul} &= 2 \left( \log_2(1 + \Gamma_{ul|fd-fd}) \right), \\ R_{fd-fd|m}^{ul} &= 2 \left( \log_2(1 + \Gamma_{ul|fd-fd}^{n \leftrightarrow m}) \right), \\ R_{fd-fd|n}^{dl} &= 2 \left( \log_2(1 + \Gamma_{dl|fd-fd}) \right), \\ R_{fd-fd|m}^{dl} &= 2 \left( \log_2(1 + \Gamma_{dl|fd-fd}^{n \leftrightarrow m}) \right). \end{aligned} \quad (12)$$

**Algorithm 1:** Constructing Crystallized Rate Region

**Data:**  $P_{max}$ ,  $P_{ul|max}$ ,  $\sigma^2$ ,  $C$ 
**Result:** Crystallized Rate Region

1. Set  $P_n = 0$ , and solve (13) for  $P_m$ ;  
Set  $P_m = 0$ , solve (13) for  $P_n$ ;
2. Set  $P_n = P_{max}$ , and solve (13) for  $P_m$ ;  
Set  $P_m = P_{max}$ , solve (13) for  $P_n$ ;
3. Set  $P_k = 0 \forall k \in [0, \dots, K_n + K_m]$ , and solve (13) for:  
 $P_m$  and  $P_n$ ;  
 $P_m$  and set  $P_n = 0$ ;  
 $P_n$  and set  $P_m = 0$ ;
4. Set  $P_n = P_m = 0$ , and solve (13) for:  
 $P_k \forall k \in [0, \dots, K_n + K_m]$ ;  
 $P_k \forall k \in [0, \dots, K_n]$  and set  $P_k = 0 \forall k \in [K_n + 1, \dots, K_n + K_m]$ ;  
 $P_k \forall k \in [0, \dots, K_m]$  and set  $P_k = 0 \forall k \in [K_m + 1, \dots, K_n + K_m]$ .
5. Construct the convex hull from points obtained in Steps 1 to 4.

### III. CRYSTALIZED RATE REGIONS

In this paper, we are interested in comparing the feasible sum rate regions achieved by the proposed model in Section II (which is obtained through power adaptation) with the crystallized rate regions for both the HD and FD networks. It must be noticed that both nodes are constrained by a maximum transmission power  $P_{max}$ . Similarly, the UL users are constrained by  $P_{ul|max}$ . Ideally speaking, in order to obtain the feasible rate, we should consider all cases of users and power allocation to the channel and each case will correspond to a point in the feasible rate region. This method is referred to as the full search method, and its complexity is exponential with respect to the number of users. In other words, the full search involves, for all possible rate values of node  $m$  rate, maximizing node  $n$  rate. Therefore, if we consider the FD-DL rate region, it can be obtained by solving the following optimization problem for all possible values of  $R_{fd-fd|m}^{dl}$ ,

$$\begin{aligned}
& \underset{P_n, P_m, \mathbf{P}_{ul}}{\text{maximize}} && R_{fd-fd|m}^{dl} \\
& \text{s.t.} && P_n \leq P_{max}, \\
& && P_m \leq P_{max}, \\
& && P_k \leq P_{ul|max} \forall k \in [1, \dots, K_n + K_m], \\
& && R_{fd-fd|m}^{dl} = R_m,
\end{aligned} \tag{13}$$

where  $\mathbf{P}_{ul} \triangleq [P_1, P_2, \dots, P_{K_m+K_n}]^T$  is a vector including all UL transmission powers.

In order to reduce the complexity of deriving the feasible rate region by solving (13), we derive the crystallized rate region instead of the full search rate region. Since the main idea of deriving the crystallized rate regions is to simplify the rate region by considering a subset of combinations which most

likely will lie on the boundary of the feasible rate region; the combinations that we will consider will be as follows

- 1) Either node  $n$  or  $m$  is silent: In that case, when node  $n$  is silent,  $P_n = 0$ ,  $P_k = 0 \forall k \in [0, \dots, K_n]$ . On the other hand, when node  $m$  is silent,  $P_m = 0$ ,  $P_k = 0 \forall k \in [0, \dots, K_m]$ . These two cases are the corner points of the feasible rate region.
- 2) Either node  $n$  or  $m$  along with their accompanied users  $K_n$  and  $K_m$  transmit at the maximum power: In that case,  $P_n = P_m = P_{max}$ ,  $P_k = P_{ul|max} \forall k \in [0, \dots, K_n + K_m]$ ,
- 3) Only DL transmissions are active: In that case,  $P_k = 0 \forall k \in [0, \dots, K_n + K_m]$ . This case will be divided into three separate subcases; the first case is when both nodes DL transmissions are active, the second case is when only node  $n$  DL transmission is active, and the third case is when only node  $m$  DL transmission is active.
- 4) Only UL transmissions are active: In that case,  $P_n = P_m = 0$ . This case will be divided into three separate subcases; the first one is when both nodes UL transmissions are active, the second one is when only node  $n$  UL transmission is active, and the third one is when only node  $m$  UL transmission is active.

The complete algorithm is explained in Algorithm 1. In the beginning, for each combination mentioned above, the transmission power constrained rate maximization problem will be solved after setting the UL and DL powers according to each case. Afterwards, the crystallized rate region will be constructed from the convex hull obtained from these rate points (as mentioned above, the convex hull is always achievable through time-sharing). It should be noticed, the number of combinations we need to consider to obtain the crystallized region is  $4N + 2$ , where  $N$  is the number of nodes in the network which is equal 2 in our model. As mentioned before, the number of combinations considered does not grow exponentially with the number of nodes and users in the network.

### IV. NUMERICAL ANALYSIS

In this section, we study and evaluate the performance of the proposed crystallized rate region and compare it with the full search, power adaptation achieved rate region. The evaluation is done under different interference conditions. The simulation setup is assumed to be two square grids. Each grid includes one node, and the users connected to that node are uniformly distributed among the grid. Unless otherwise stated, the following simulation parameters are used in the numerical analysis:  $P_{max} = 2W$ ,  $P_{ul|max} = 0.1W$ ,  $\alpha = 3$ ,  $M = 4$ ,  $\sigma = -80dB$ , and  $C = 10^{-8}$ .

Fig. 2 shows the sum DL and UL rate region for both FD and HD modes. It should be noticed that the results shown in Fig. 2 are generated in a high interference scheme. However, in spite of that high interference level, FD transmission was able to maintain a better rate region than that achieved by HD transmission. Additionally, when comparing the full search rate region and the crystallized region, it can be noticed that

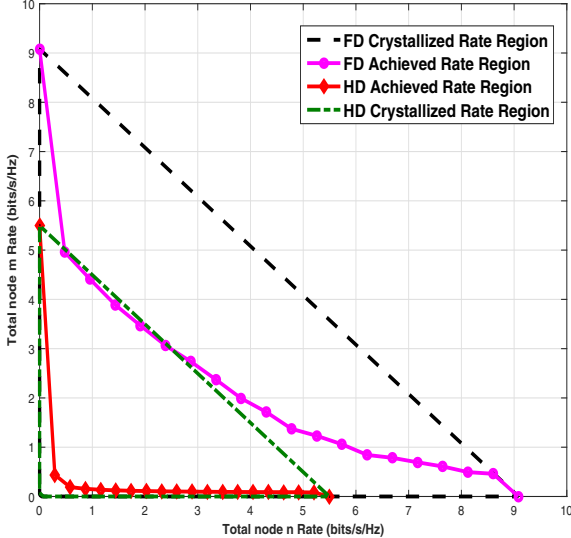


Fig. 2: Achieved and Crystallized Total DL and UL Rate Regions for HD and FD Modes

the crystallized rate region is able to include 100% of the full search region with much less complexity. In other words, all the points in the full search rate HD and FD regions are achievable in the crystallized HD and FD rate regions, respectively. From the results in Fig. 2, it is clear that for high interference regime, in order to obtain better rate duo for nodes  $n$  and  $m$ , utilizing time sharing between points on the derived crystallized rate region will result in higher rates that can not be achieved by power adaption.

Furthermore, Fig. 3 shows the achieved full search UL rate regions for both the HD and FD modes for high interference transmission. First, it is noticed that the FD transmission achieves better rate region than the HD transmission. Second, it is clear that the crystallized UL regions for both the FD and HD transmissions can achieve 100% of the full search rate region. In other words, all the points in the full search rate HD and FD regions are included in the crystallized HD and FD rate regions, respectively. Similarly, from the results in Fig. 3, it is clear that for high interference regime, in order to obtain better rate duo for nodes  $n$  and  $m$ , utilizing time sharing between points on the derived crystallized rate region will be better than power adaption.

Fig. 4 shows the DL achieved rate region and the crystallized DL achieved rate region for FD transmission. It should be mentioned that, in the results presented in Fig. 4, the model is simulated for low interference regime. The interference was adjusted by increasing the distances between users in a way to decrease the interference introduced from the UL transmissions. Furthermore, it can be verified from the results in Fig. 4, that the crystallized region gives a good approximation for the full search achieved rate region. In case of  $P_{max} = 10W$ , the crystallized region achieved almost 97% of the full search

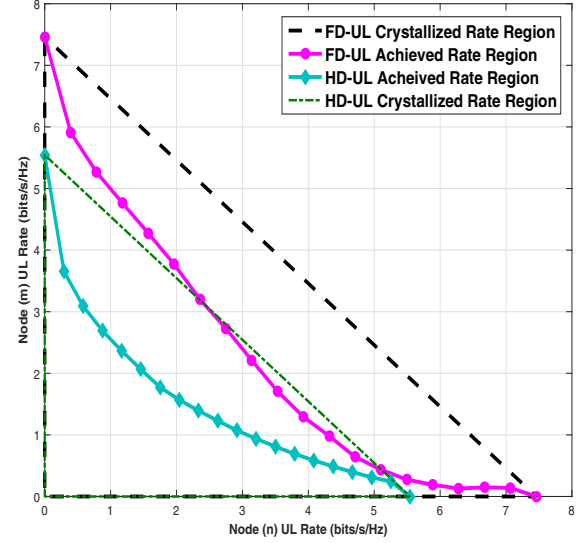


Fig. 3: Achieved and Crystallized UL Rate Regions for HD and FD Modes

region. Additionally, in case of  $P_{max} = 2W$ , the crystallized region achieved about 96% of the full search region. Finally, as expected, increasing the maximum allowed DL power  $P_{max}$ , the achieved and the crystallized rate regions will become larger.

Finally, Fig. 5 shows the achieved and crystallized rate region for DL-FD transmission. The interference conditions in Fig. 5 are different from that in 4, and that explains the switching between the weak interference transmission for large values of nodes  $m$  DL rate, and strong interference transmission for small values of node  $m$  DL rate. For weak interference transmission, the crystallized region attains almost 99% of the full search achieved rate region, and for the strong interference transmission, the crystallized region achieved 100% of the full search achieved rate region. From the results in Fig. 5, when  $R_{fd-fd|n}^{dl}$  changes from  $R_{fd-fd|n}^{dl} = 0 \text{ bits/s/Hz}$  to  $R_{fd-fd|n}^{dl} = 13 \text{ bits/s/Hz}$ , and correspondingly,  $R_{fd-fd|m}^{dl}$  changes from  $R_{fd-fd|m}^{dl} = 37 \text{ bits/s/Hz}$  to  $R_{fd-fd|m}^{dl} = 33 \text{ bits/s/Hz}$ , respectively, the loss in performance from utilizing time sharing between these two rate duos on the crystallized region is very small when compared to the full search region. However, as  $R_{fd-fd|n}^{dl}$  grows larger, it will be more preferable to use time sharing rather than power adaptation.

## V. CONCLUSION

In this paper, a small cell network with two full-duplex enabled node is studied. Based on the derived received rates for both nodes, the rate maximization problem is formulated to derive the achieved rate region and a very low complexity algorithm is proposed to obtain the crystallized rate region. The idea is to consider a certain set of points that most probably will lie on the rate region boundary and construct their convex hull.

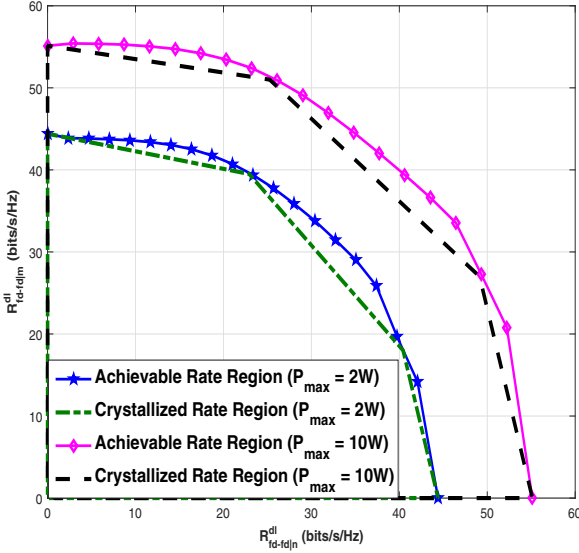


Fig. 4: Achieved and Crystallized DL Rate Regions for FD Mode for  $P_{max} = 2W$  and  $P_{max} = 10W$

From the numerical results, the effectiveness of the proposed crystallized rate region in approximating the full search rate region, for different interference conditions, is validated. In case of high interference transmission, the crystallized region is able to fully include all points in the full search region. On the other hand, in case of low interference transmission, the crystallized region offers a very accurate approximation for the full search region. Also, in some cases, the derived crystallized rate regions will enclose the full-search, power adaptation derived region; this means that time-sharing between points on the derived crystallized rate region can achieve rate points that can never be achieved through power adaptation.

## REFERENCES

- [1] M. Duarte and A. Sabharwal, "Full-duplex wireless communications using off-the-shelf radios: Feasibility and first results," in *IEEE Conference Record of the Forty Fourth Asilomar Conference on Signals, Systems and Computers (ASILOMAR)*, Pacific Grove, CA, Nov. 2010, pp. 1558 – 1562.
- [2] D. Bharadwaj, E. McMillin, and S. Katti, "Full duplex radios," in *SIGCOMM*, Hong Kong, China, Aug. 2013, pp. 375–386.
- [3] M. Jain, J. I. Choiy, T. M. Kim, D. Bharadwaj, S. Seth, K. Srinivasan, P. Lewis, S. Katti, and P. Sinha, "Practical, real-time, full duplex wireless," in *MobiCom*, Las Vegas, NV, Sep. 2011, pp. 301–312.
- [4] Z. Ma, Z. Zhang, Z. Ding, P. Fan, and H. Li, "Key techniques for 5G wireless communications: network architecture, physical layer, and MAC layer perspectives," *Science China Information Sciences*, vol. 58, no. 4, pp. 1–20, 2015.
- [5] Z. Zhang, X. Chai, K. Long, A. V. Vasilakos, and L. Hanzo, "Full duplex techniques for 5G networks: self-interference cancellation, protocol design, and relay selection," *IEEE Communications Magazine*, vol. 53, no. 5, pp. 128–137, May 2015.
- [6] L. Song, R. Wichman, Y. Li, , and Z. Han, *Convex Optimization Full-Duplex Communication*. in print, Cambridge University Press, UK.
- [7] R.-A. Pitaval, O. Tirkkonen, R. Wichman, K. Pajukoski, E. Lahetkangas, and E. Tiirola, "Full-duplex self-backhauling for small-cell 5G networks," *IEEE Wireless Communications*, vol. 22, no. 5, pp. 83–89, Oct. 2015.
- [8] T. Q. Quek, G. de la Roche, İ. Güvenç, and M. Kountouris, *Small cell networks: Deployment, PHY techniques, and resource management*. Cambridge University Press, Jan. 2013.
- [9] J. Hoydis and M. Debbah, "Green, cost-effective, flexible, small cell networks," *IEEE Communications Society MMTC*, vol. 5, no. 5, pp. 23–26, 2010.
- [10] R. Sultan, L. Song, and Z. Han, "Impact of full duplex on resource allocation for small cell networks," in *IEEE Global Conference on Signal and Information Processing (GlobalSIP)*. IEEE, Dec. 2014, pp. 1257–1261.
- [11] R. Sultan, L. Song, K. G. Seddik, and Z. Han, "Full-duplex meets multiuser mimo: Comparisons and analysis," *IEEE Transactions on Vehicular Technology*, no. 99, Mar. 2016.
- [12] R. Sultan, L. Song, K. G. Seddik, Y. Li, and Z. Han, "Mode selection, user pairing, subcarrier allocation and power control in full-duplex ofdma hetnets," in *2015 IEEE International Conference on Communication Workshop (ICCW)*. IEEE, Sep. 2015, pp. 210–215.
- [13] W. Bi, X. Su, L. Xiao, and S. Zhou, "On rate region analysis of full-duplex cellular system with inter-user interference cancellation," in *IEEE International Conference on Communication Workshop (ICCW)*, London, UK, Jun. 2015, pp. 1166–1171.
- [14] D. Korpi, T. Riihonen, and M. Valkama, "Achievable rate regions and self-interference channel estimation in hybrid full-duplex/half-duplex radio links," in *49th Annual Conference on Information Sciences and Systems (CISS)*, Baltimore, MD, Apr. 2015.
- [15] W. Li, J. Lilleberg, and K. Rikkinen, "On rate region analysis of half- and full-duplex OFDM communication links," *IEEE Journal on Selected Areas in Communications*, vol. 32, no. 9, pp. 1688–1698, Jun. 2014.
- [16] M. Charafeddine, Z. Han, A. Paulraj, and J. Cioffi, "Crystallized rates region of the interference channel via correlated equilibrium with interference as noise," in *IEEE International Conference on Communications*, Germany, Aug. 2009.
- [17] M. A. Charafeddine, A. Sezgin, Z. Han, and A. Paulraj, "Achievable and crystallized rate regions of the interference channel with interference as noise," *IEEE Transactions on Wireless Communications*, vol. 11, no. 3, pp. 1100–1111, Mar. 2012.
- [18] R. Raghavendra, H. Zou, M. Charafeddine, Z. Han, and J. M. Cioffi, "Low complexity multi-user rate region maximization for frequency-selective interference channel," in *Proceedings of the 6th International Wireless Communications and Mobile Computing Conference*, 2010, pp. 392–396.

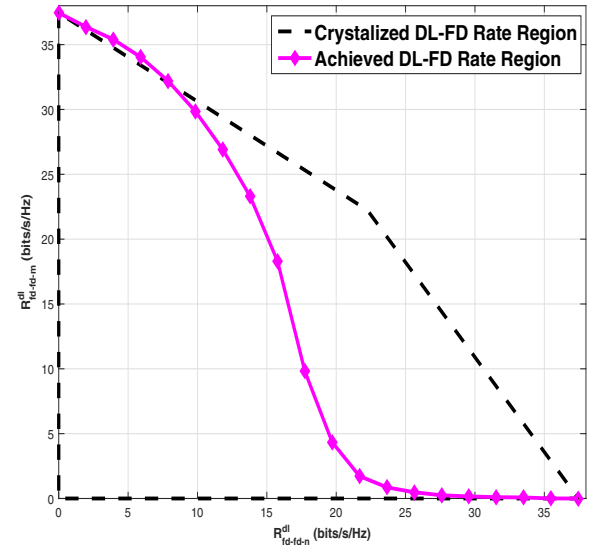


Fig. 5: Achieved and Crystallized DL Rate Regions for FD Modes